Photochemical Exploration of Reaction Dynamics at Catalytic Metal Surfaces: From Ballistics to Statistics

IAN HARRISON

Department of Chemistry, University of Virginia, Charlottesville, Virginia 22901

Received January 23, 1998

1. Introduction

Surfaces form the working template upon which much of the world's technologically important chemistry occurs.[1] Catalysis, corrosion, adhesion, friction/lubrication, and materials growth all depend critically upon interfacial chemistry. This account discusses how photochemical methods can be exploited to explore the fundamental dynamics of elementary catalytic reactions occurring at the gas/metal interface.[2] By studying reactions on single crystal surfaces, several rather unique opportunities arise. The first stems from the natural self-organization of adsorbed molecules which become stereochemically arranged by the periodic surface forces. By initiating reactions nonthermally at low temperatures, one may investigate restricted and organized reactive geometries. Second, in contrast to reactions occurring in bulk condensed phases, characterization of nascent product state distributions for surface reactions is readily achieved through gas phase spectroscopy if the products are promptly desorbed. Studies of such surface reactions can provide us with a dynamical window into the world of condensed phase reactions. Finally, the remarkable ability of the scanning tunneling microscope (STM) to image and manipulate atoms and molecules currently permits nonthermal reactions to be examined microscopically at the level of individual reagents adsorbed at specific surface sites.[3] In the long run, we must anticipate that surfaces will prove to be among the very best places to study the elementary details of chemical reactions.

Much of our dynamical information about surface reactions derives from molecular beam and recombinative thermal desorption studies of reactions carried out on single crystal surfaces prepared in ultrahigh vacuum.[4] State analysis of products desorbed into the gas phase has come from time-of-flight (TOF) spectroscopy to a quadrupole mass spectrometer, infrared chemiluminescence, laser induced fluorescence, or resonance enhanced multiphoton ionization. Unfortunately, most catalytic reactions, such as CO oxidation, proceed through the Langmuir−Hinshelwood (L−H) mechanism in which thermalized adsorbed reagents react at the surface temperature (e.g. $^1/_2O_2(g) + CO(g) \rightarrow O(ad) + CO(ad) \rightarrow CO_2(g)$). The energetic monochromaticity of reagent molecular beams goes largely to waste for such L−H reactions, but this may not be the case for reactions proceeding through the Eley−Rideal (E−R) mechanism in which an impinging gas phase species reacts directly with an adsorbate. Despite their long standing discussion, Eley−Rideal reactions have only recently been definitively observed when radical species such as H atoms were made incident on adsorbate covered surfaces.[5] Cross-sections for radicals reacting with closed shell species are generally much greater than those for reactions involving two closed shell species because the reduced Pauli repulsion experienced during reactive approach of a radical allows for much lower activation barriers.[6] Just as for gas phase reactions,[7] it is only practically feasible to study the *dynamics* of state-prepared radical/closed shell or radical/radical surface reactions which occur with relatively high probability upon every interreagent collision. In the case of typical L−H reactions, at least one of the closed shell molecular reagents incident from the gas phase is dissociated on the surface to give an adsorbate whose reactivity lies somewhere intermediate between a radical and closed shell species (e.g. $O_2(g) \rightarrow 2O(ad)$ during CO oxidation).[1] This reactivity is typically insufficient to generate a L−H reaction upon every interreagent collision on the surface, at least not after the dissociated fragments of the molecular reagent have become thermalized to the surface temperature. However, prior to thermalization, the "hot" molecular fragments may display an enhanced reactivity before their heat of adsorption is dissipated. Reactions of such "hot precursors" to the thermalized L−H reagents through a mechanism intermediate between the E−R and L−H mechanisms were first discussed by Harris and Kasemo[8] to explain low-temperature reactions occurring when H_2 and O_2 gases were adsorbed on a polycrystalline Pt foil. Hot H atom fragments liberated by thermal dissociation of adsorbing H_2 were suggested to react with adsorbed O and OH species to form OH and H_2O products through a precursor (or H−K) mechanism. Analogous surface photochemical reactions involving hot photofragments produced by adsorbate photofragmentation were first demonstrated on insulators by Polanyi's group at Toronto[9] and on metals by Ho's group at Cornell.[10]

Photochemical methods for exploring reaction dynamics on metals have been somewhat delayed in developing because of the popular perception that electronic quenching rates for adsorbates on metals were prohibitively fast for surface photochemistry to be observable.[11] It is only over the past decade that adsorbate photochemistry on metals has begun to be identified and examined in detail.[12] Adsorbed molecules on a metal may be excited directly by light absorption or indirectly by interaction

Ian Harrison was born in Montreal, Canada, in 1959. He joined the faculty at Virginia in 1989 after a Ph.D. with John Polanyi at the University of Toronto and a postdoctoral fellowship with Gabor Somorjai at Berkeley. His current research focuses on the study of surface reaction kinetics and dynamics using laser and STM techniques.

10.1021/ar9700926 CCC: $15.00
Published on Web 07/17/1998

with photoexcited charge carriers of the substrate. Rapid quenching of electronically excited adsorbate states at metals ($\tau \sim 1-10$ fs) makes the quantum yield for observable adsorbate photochemistry very small. Direct absorption of UV light by an adsorbate monolayer is relatively improbable (ca. 0.01%), but the metal can absorb and gather much of the incident UV light (ca. 50%) close to the surface where hot carriers may reach the adsorbate. Furthermore, gas phase photochemical cross-sections are several orders of magnitude smaller than the larger electron−molecule cross sections for dissociative electron attachment (DEA) [e.g. 100 Å^2 for DEA of CCl_4(g)!]. As a consequence, adsorbate photochemistry on metals is usually driven by photoexcited substrate electrons. Observed photochemistry has included photoconversion between adsorbate states, photodesorption, photofragmentation, and photoreaction. Although these broad features of adsorbate photochemistry on metals are well-established,[11−13] the study of adsorbate photochemical dynamics remains an active and rapidly growing field of scientific investigation.[14]

A particular interest at Virginia has been to exploit adsorbate photochemistry to investigate the dynamics of catalytic reactions on metal single crystals.[15] Ideally, photofragmentation induced within an ordered submonolayer of coadsorbates can lead to reactive attack of the photofragments on neighboring coadsorbed molecules. The range of impact parameters and relative orientations of attack are constrained by the initial bonding of the coadsorbates to the surface. The dynamics of such "surface aligned photoreactions",[9,16,17] can be followed by TOF techniques if the photoproducts leave the surface promptly and the reactions are initiated with pulsed lasers. By working at low temperatures and under ultrahigh vacuum conditions, the initial state of the adsorbates can be characterized using surface analytical techniques. By initiating the photoreaction with a tunable laser, the experimenter may vary the translational and internal energy distributions of the photofragments involved in the reactive collisions, while the collisional stereochemistry may be modulated by varying the coverage of the coadsorbed precursors.

The rapid quenching of electronically excited adsorbate states on metals ($\tau \leq 10$ fs) means that bimolecular reactions involving photofragment are likely to proceed, for the most part, along the ground state potentials relevant to catalysis. As a consequence, studies of photochemical model systems may provide insight as to the dynamics and mechanisms of related catalytic reactions which are normally thermally driven. In this account, experimental studies relevant to O_2 chemistry, CO oxidation, and C−H bond cleavage of methane on Pt(111) are discussed and connections are made to developing theories of surface reactivity. Our analysis of these reactions will range from one considering simple collisional ballistics to reactive statistics.

2. Oxygen Photochemistry on Platinum(111)

Much of the photochemistry of O_2 on Pt(111) can be understood on the basis of the ground state potential

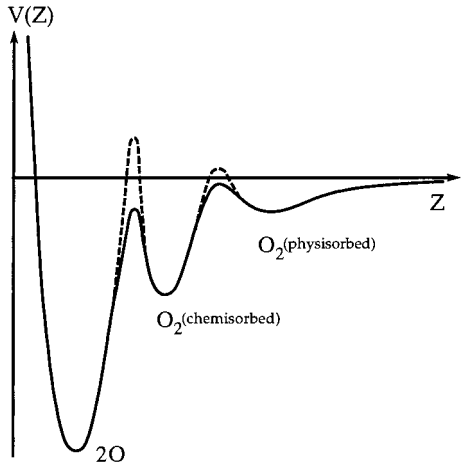

FIGURE 1. (Solid curve) Schematic 1-D depiction of the O_2/Pt(111) potential along the minimum energy pathway leading to dissociative adsorption as determined by low-T_s adsorption/desorption experiments. Effective energetic barriers sampled in molecular beam adsorption and high-T_s desorption experiments are represented by the dashed curves.

energy surface (PES) displayed in Figure 1 for which the O_2 chemisorbed state is separated from the atomic and physisorbed states by heavily constrained transition states.[18,19] Under ultraviolet irradiation, chemisorbed O_2 on Pt(111) undergoes parallel photorearrangement, photodesorption, and photofragmention.[20] All of the chemisorbed O_2 photochemistry is believed to result from the transient capture of a photoexcited substrate electron into the 3 σ_u* orbital of chemisorbed O_2.[21,22] The transient O_2^- is attracted toward the surface by the image potential and the equilibrium bond length is lengthened. Rapid neutralization of the anion in close proximity to the metal surface results in a translationally and vibrationally excited neutral molecule which can go on to diffuse, desorb, or dissociate on the ground state PES. Similar photoactivity was observed for physisorbed O_2.[22] The 308 nm photodesorption dynamics of both physisorbed and chemisorbed O_2 were probed in our laboratory by laser triggered TOF spectra to a twice differentially pumped mass spectrometer such that angular yield distributions, $P(\vartheta)$, and translational energy distributions, $P(E_T)$, could be derived.[22] Photodesorption from the chemisorbed state was characterized by a desorbate mean translational energy of $\langle E_T \rangle = 0.12$ eV (comparable to a "temperature" of $\langle E_T \rangle / 2k_b = 700$ K) and a roughly cosine angular distribution consistent with partial trapping/thermalization of the photoexcited O_2 in the ground state chemisorption well prior to desorption. By contrast, photodesorption from the physisorbed state produced a desorbate $\langle E_T \rangle = 0.30$ eV (∼1750 K) and a much sharper ($0.9 \cos^{34} \vartheta + 0.1 \cos \vartheta$) angular distribution indicative of more direct desorption dynamics.

3. Ballistic Collisions of Hot Oxygen Atom Photofragments

If O atom photofragments are to be used as reagents in dynamical studies of bimolecular surface reactions, it will

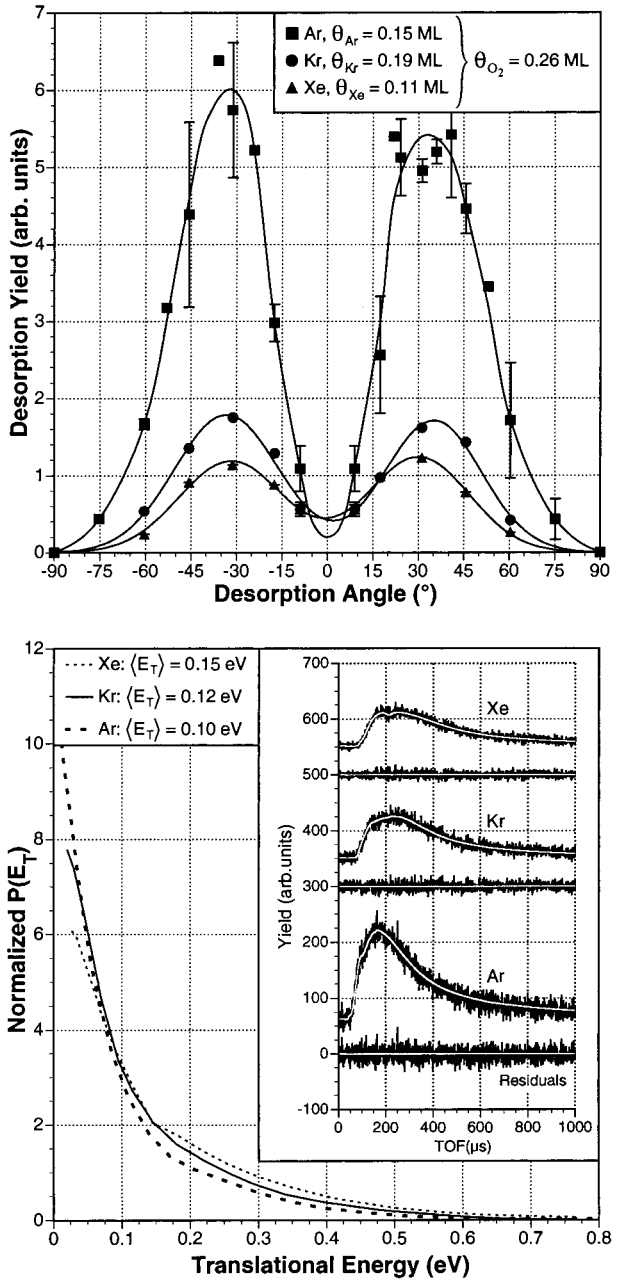

FIGURE 2. (a, top) Angular distributions of desorbing Ar, Kr, and Xe from coadsorbed ~0.15 monolayer noble gas/0.26 monolayer chemisorbed O_2/Pt(111) surfaces irradiated at 250 nm. (b, bottom) TOF spectra and translational energy distributions for Ar, Kr, and Xe desorbing into $\vartheta = 35°$.[23] The $P(E_T)$ distributions were forward simulated over the experimental parameters to obtain the smooth fits to the TOF spectra.

be necessary to have a measure of their energy. Unfortunately, the O atoms produced by O_2 photofragmentation on Pt(111) do not leave the surface, so TOF techniques cannot *directly* quantify the O atom translational energies. Nevertheless, it has been possible to *indirectly* quantify the photofragment energies by coadsorbing a series of noble gases (Ar, Kr, and Xe) with O_2 and monitoring the TOF spectra and angular yield of the noble gases which are desorbed via collisions with ballistic O atom photofragments.[23] The collisionally desorbed noble gases leave the 20 K surface in a narrow range of angles close to $\vartheta =$

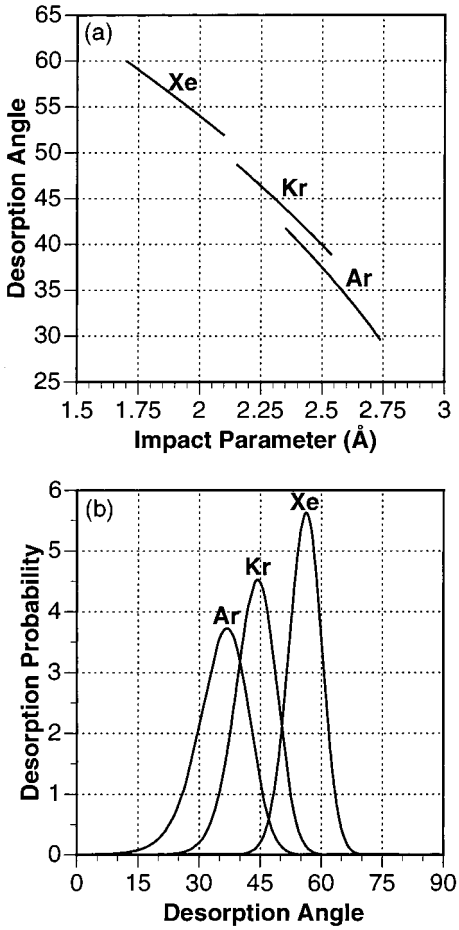

FIGURE 3. (a) Impact parameter versus calculated noble gas desorption angle in O atom photofragment collisions with Ar, Kr, and Xe. (b) Simulated noble gas angular distributions based on hard sphere scattering around a Gaussian range of impact parameters (b_0, D fixed by literature values; $\sigma_b = 0.2$ Å).

35° and with mean translational energies in the 0.12 eV (1400 K) range (see Figure 2). The desorption dynamics indicate that the O atoms chatter between the heavier departing noble gas atoms and the underlying surface. A lower bound of 0.73 eV was established for the energy of the fastest O atom photofragments produced by irradiation at 250 nm.

Hard sphere elastic scattering theory for this system leads to the simple result that the noble gases should desorb at $\vartheta = \cos^{-1}(b/D)$, where b is the impact parameter and D is the collision diameter. Chemisorbed O_2 is adsorbed with an internuclear bond parallel to the surface and launches O atom photofragments toward the noble gases, which are physisorbed about 1.7−2.7 Å further away from the surface plane. The desorption angular distribution can be simply modeled under the assumption that thermal vibrations of the reagents against the surface lead to a Gaussian distribution of impact parameters,

$$P(\vartheta) = \frac{D \sin(\vartheta)}{\sigma_b [2\pi]^{1/2}} \exp\left\{ - \frac{(D \cos(\vartheta) - b_0)^2}{2\sigma_b{}^2} \right\}$$

Figure 3 shows the mapping of impact parameters into desorption angles and the desorption angular distributions

predicted for scattering by a *single collision* in the plane of the detector. The mean energy transfer to the different noble gases at the most probable desorption angles should be 0.27 ± 0.01 given literature impact parameters and the calculated ϑ's. Comparing Figure 3 to the experimental data of Figure 2, it is clear that only the Ar desorption is roughly consistent with the single collision predictions. The heavier noble gases desorb at overly small angles and have far too much translational energy, particularly so because their adsorption energies are significantly larger than Ar's! We believe that chattering of the light O photofragments between the heavier noble gases and the heavy surface leads to multiple collisions and enhanced energy transfer.[23,24] A lower bound of 0.73 eV for the energy of the fastest O atom photofragments could be established by the sum of the Xe adsorption energy (E_{ad} = 0.29 eV) and the translational energy of the fastest desorbing Xe (5% had $E_T \geq 0.44$ eV). A less conservative estimate of the O atom translational energy distribution would be to assume single collision dynamics for the Ar desorption, neglect the Ar adsorption energy, and scale the 35° $P(E_T)$ for Ar by the calculated energy transfer of 27%. These energies are in the range of the 1.1 ± 0.1 eV calculated to be available to O atoms from thermal dissociation of chemisorbed O_2 on Pt(111). Recent low-temperature STM measurements also indicate that thermal[25] and nonthermal dissociation[26] of chemisorbed O_2 on Pt(111) produce hot O atoms of similar energies which can travel several lattice spacings across the surface.

4. CO Oxidation on Platinum(111)

The high-temperature oxidation of CO on platinum is relatively well-understood and finds extensive application in the catalytic converters of automobiles and industry.[1] At temperatures above 200 K, CO oxidation occurs as coadsorbed CO and O atoms react in the L−H fashion. The energetics of the low coverage oxidation on Pt(111) were established by molecular beam experiments[27] and are illustrated in Figure 4. The energetic position of the molecularly adsorbed reagents lies a scant 0.04 eV below that of the $CO_2^{\ddagger}$ transition state for the L−H reaction. As a consequence, when coadsorbed CO and O_2 are heated to 150 K and O_2 thermally dissociates to yield hot O atoms with nascent energies of ~1.1 eV, it is believed that some of the initial O + CO collisions are sufficiently energetic to traverse the $CO_2^{\ddagger}$ transition state barrier and produce product via a H−K reaction mechanism.[28] The dynamics of the low-temperature H−K reaction are quite similar to those of the high-temperature L−H reaction, which supports the notion of passage through a common transition state. The transition state is believed to be an O atom coupling to a CO molecule with an obtuse included angle in a configuration somewhere intermediate between bent CO_2^- and linear CO_2. The CO_2 product dynamics are characterized by a $\sim\cos^8 \vartheta$ angular distribution and mean translational energies in the 0.36−0.6 eV range.[28] Differences in the product $\langle E_T \rangle$s have been attributed to differing reagent coverages which influence the reaction path

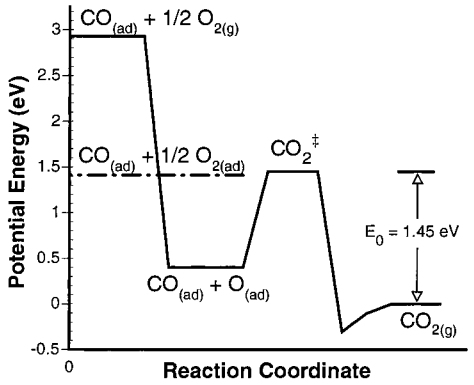

FIGURE 4. Potential energy diagram for catalytic oxidation of CO on Pt(111). The solid curve is derived from molecular beam scattering data obtained at low coverages and high temperatures.[27] The potential energy of molecularly adsorbed reagents is given by the dashed line.

energetics. The activation barrier for the L−H reaction between adsorbed O atoms and CO falls from 1.05 to 0.51 eV as the O atom coverage (θ_O) is increased from zero to $\theta_O \geq 0.1$ monolayer.[27]

Menzel and co-workers[28] have pointed out that the reagent adsorption energies are relatively independent of coverage, so a reduction in the L−H activation barrier signals a reduction in the exit channel exoergicity, E_0, from the $CO_2^{\ddagger}$ transition state to CO_2(g). Under this assumption, the fraction of the available product energy channeled into translation, $f_T = \langle E_T \rangle / E_0$, is found to be fairly constant at $f_T \sim 40\%$. Infrared chemiluminescence experiments on Pt foil have shown that the CO_2 product from the high-temperature L−H reaction is excited to a mean rovibrational energy of $\langle E_{RV} \rangle = 0.36$ eV.[29] The fraction of the available product energy appearing in molecular internal energy under these conditions is $f_{RV} \sim 40\%$. If product energy partitioning is fairly independent of coverage and $f_{RV} \sim 40\%$ and $f_T \sim 40\%$, then we may estimate the fraction of the product energy that is taken up by the surface degrees of freedom as $f_S \sim 20\%$.[28]

The first dynamical study of a bimolecular photoreaction on a metal surface was carried out at Virginia for the CO photooxidation reaction on Pt(111).[16] Figure 5 shows the TOF spectrum and associated translational energy distribution for the CO_2 photoproduct from the 308 nm excimer laser induced photochemical reaction between chemisorbed O_2 and CO on a Pt(111) surface held at T_s = 25 K. The CO_2 angular distribution was sharply peaked (full width at half-maximum (fwhm) ~ 20°) around the surface normal. The mean CO_2 translational energy into $\vartheta = 0°$ was $\langle E_T \rangle = 0.45$ eV and the maximum translational energy was $E_{Tmax} = 1.35 \pm 0.15$ eV. The photochemical reaction dynamics are remarkably similar to those discussed above for the high-temperature L−H and the low-temperature H−K reactions. The near coincidence of the limiting CO_2 photoproduct translational energy with the thermal reaction's exit channel exoergicity ($E_0 = 1.45$ eV in the low θ_O limit) and the surface normal peaked product angular distribution argue for passage through similar transition state configurations with similar energies for

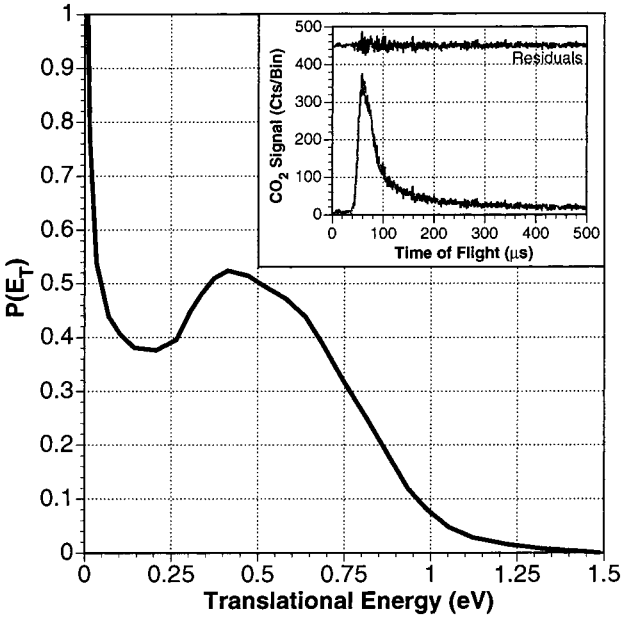

FIGURE 5. TOF spectrum and translational energy distribution for CO_2 photoproduct detected at $\vartheta = 0°$ after 308 nm irradiation of 0.12 monolayer CO/0.12 monolayer O_2/Pt(111).[16]

both the thermal and photochemical reactions. Although the chemisorbed O_2 was photoexcited by 4.03 eV photons at 308 nm, it seems that rapid quenching of the charge transfer excited O_2^- species leads to a modestly energized or hot O_2 species in its electronic ground state, which can go on to desorb, dissociate, or react as would a thermally energized O_2 on the PES of Figure 1 or 4. Further experimental support for this viewpoint comes from the photodesorption dynamics of chemisorbed O_2 discussed earlier. Ultimately, it is the photochemically produced hot O atoms which are believed to oxidize the CO.[10]

In general, we should anticipate that the rapid electronic quenching rates on metals will ensure that surface photochemical reactions will proceed, for the most part, on the ground state potentials relevant to catalysis. Even for particularly energetic photoreactions involving relatively light reactive species such as O atom or CH_3 radical photofragments with as much as 2 eV of translational energy, the fragments will move less than 0.3 Å over a typical excited state lifetime of less than 5 fs for a chemisorbed species.[30]

The rapid quenching of adsorbate electronic states on metals also serves to damp the generation of photoproduct translational and internal energy on the photochemically excited PES. Zimmermann and Ho[30] have shown that typical photoproduct translational energy distributions evolved on relatively featureless model PESs should have the form of flux weighted Maxwell−Boltzmann distributions with high "temperatures" (e.g. 1000 K) related to the excited state lifetime and some parameters of the ground and excited state PESs. Ultimately, the rapid electronic quenching of adsorbates on metals may be advantageous to photochemists interested in bimolecular reaction dynamics on surfaces since this property tends to (i) require that photochemically initiated reactions will proceed primarily on the ground state potentials and (ii) suggest that photochemically energized reagents may be treated as locally hot reagents even though the surface and surrounding species may remain cold.

We apply these last principles to comment on the CO oxidation dynamics and PES with reference only to the CO_2 photoproduct translational energy distribution of Figure 3. The limiting translational energy of $E_{Tmax} = 1.35 \pm 0.15$ eV provides an estimate for the exit channel exoergicity, E_0. The idea here is that for small dynamical systems such as the CO_2/Pt(111) transition state there should be at least some reactive trajectories for which all the product energy appears as pure translation. This principle is commonly applied in gas phase photofragment translational energy spectroscopy to extract bond dissociation energies for small molecules (by assuming that $D_0 = h\nu - E_{Tmax}$).[31] The complication in surface photochemical reactions is that the reagents may have energies in excess of that required to surmount the activation barrier for reaction, and some of this excess energy may be channeled into product translation. However, in common with thermal reactions, the reagent energy distribution is expected to be exponentially damped with increasing energy (i.e. $P(E) \sim \exp(-E/k_bT^*)$, where T^* is an effective temperature resulting from rapid quenching on the excited state potential), so the majority of successful reactive trajectories will be very close in energy to the transition state barrier. For reactions with relatively large exit channel barriers (i.e. $E_0 \gg k_bT^*$) the approximation that $E_0 \sim E_{Tmax}$ may be fairly good.[32] If we accept this line of reasoning for the CO photooxidation reaction, we may also estimate the average partitioning of product energy into translation as $f_T = \langle E_T \rangle / E_0 \sim 0.45$ eV/1.35 eV = 33% which compares to an average value of 40% for the thermal L−H reaction and a value as low as 25% for the thermal H−K reaction.[35]

The dynamics of the CO photooxidation are consistent with a mechanism involving reactive attack of hot O atom photofragments on nearby CO. Although we have argued above that laser excitation of chemisorbed O_2 acts much like a pulsed Bunsen burner to locally heat the O_2 species and liberate reactive O atom "photofragments", it may be possible to vary the O atom translational energy distribution by photoexciting the chemisorbed O_2 at different wavelengths to access different Franck−Condon regions of the charge transfer excited state. It might then be possible to examine the effect of reagent translational energy on the CO photooxidation reactivity and dynamics.

5. C−H Bond Activation of Methane: Dissociative Adsorption on Platinum(111)

Interest in methane C−H bond activation and cleavage on transition metal surfaces stems from the desire to optimize catalytic methods to convert this abundant natural gas resource into higher order hydrocarbons and liquid chemical feedstocks. Our photochemical approach for examining $CH_4(g) \leftrightarrow CH_3(ad) + H(ad)$ reactions on Pt(111) was to explore the dynamics of methyl radical hydrogenation directly and to use microscopic reversibility

and detailed balance arguments to learn about methane dissociative adsorption. Methyl radical hydrogenation was examined by 308 nm excimer laser irradiation of a CH_3-Br/H/Pt(111) surface held at 20 K.[17] Photoinduced dissociative electron attachment (DEA) of hot substrate electrons to CH_3Br led to hot CH_3 radicals which abstracted surface H to form methane. Photoproduct methane left the surface in a sharp ($0.8 \cos^{30} \vartheta + 0.2 \cos \vartheta$) angular distribution and with a high mean translational energy, $\langle E_T \rangle = 0.45$ eV. The peaked shape of the methane $P(E_T)$ provided evidence for an exit channel barrier which directed substantial energy into product translation. Microscopic reversibility implies that an entrance channel barrier should be surmounted in the reverse reaction, methane dissociative adsorption. In the photochemical hydrogenation reaction, methyl radicals were produced with translational energies of up to 2 eV,[33] and the reactive trajectories may have sampled a portion of the reactive potential somewhat differently than in a thermal reaction. As a consequence, it was instructive to examine the thermal hydrogenation, $CH_3(ad) + H(ad) \rightarrow CH_4(g)$, by angle resolved thermal programmed reaction (TPR), where detailed balance should apply.[34] Adsorbed CH_3 radicals were produced by photoinduced DEA of CH_3Br for which about 20% of the methyl photofragments became trapped on the surface. Methane produced by TPR left the surface in a $\cos^{37} \vartheta$ angular distribution at $T_s = 240$ K. The sharply peaked methane angular distribution provided further evidence for a large exit channel barrier. Kinetic isotope effects for both the photochemical and thermal hydrogenation reactions provided no evidence for tunneling ($k_H/k_D \leq 1.5$), contrary to the predictions of the often discussed thermally assisted tunneling model[35] for methane dissociative adsorption. These low kinetic isotope effects led to our development of an alternative "over-the-barrier" model for $CH_4(g) \leftrightarrow CH_3(ad) + H(ad)$ reactions based on statistical, microcanonical rate theory.[36]

Molecular beam studies[35a,37] of methane dissociative adsorption on Pt(111) show that dissociative sticking increases monotonically with methane internal energy, normal translational energy, and the surface temperature. Apparently, energy in all these modes can help an impacting methane molecule overcome the ~0.65 eV barrier to dissociative adsorption. Given that the time scale for an energetic collision of a methane molecule with the surface is $\tau_c \sim 10^{-13}$ s and the speed of sound in Pt is 3.3×10^3 m/s, only local surface atoms in the topmost layer may exchange vibrational energy with the molecule (i.e. within a radius of ~3.3 Å). This deduction allows us to focus our attention on an energized molecule/surface complex involving only a few surface atoms. If we assume that electronic energy exchange between the surface and molecule can be neglected, since methane has no low-lying electronically excited states, then we may model the surface reaction in analogy to an adiabatic gas phase reaction between a molecule and a cluster of surface atoms. If we further assume that energized molecule/surface complexes statistically span their phase space as a collisionally excited ensemble, then the well-established RRKM methods of unimolecular rate theory should be applicable. Importantly, we do not need to require that each individual energized complex statistically explore its phase space in the short $\tau_c \sim 100$ fs allotted for a surface collision. It suffices that the ensemble of collisionally prepared complexes spans this phase space in order for the statistical kinetic methods to work. The latter requirement is much less restrictive and more likely since the initial conditions (i.e. collisional impact parameters and orientational and vibrational phases) are not well-specified in a beam experiment. Even a modestly mixing reactive potential may serve to diverge the trajectories of the incident molecules sufficiently to generate a fairly statistical array of energized complexes. These assumptions allow for the development of a microcanonical rate theory model which can treat *direct* dissociative sticking of polyatomic molecules under both equilibrium and non-equilibrium conditions.[36]

The statistical model for methane dissociative adsorption assumes a loose transition state, C−H stretch as the reaction coordinate and conservation of incident molecular momentum parallel to the surface. Ultimately there are only three free parameters: the reaction barrier height, the methane−Pt(111) vibrational frequency, and the number of active Pt vibrational modes in the energized complex. Simulations to a single set of molecular beam sticking data defined these parameters as $E_0 = 0.635 \pm 0.1$ eV, $\nu = 130 \pm 30$ cm^{-1}, and $n = 3$, respectively.[36] The remaining molecular beam sticking data which probed the effects of methane translational and internal energies, isotope, and surface temperature are predicted quite well, as illustrated in Figure 6. Notice that, in the nonequilibrium molecular beam experiments, the "Arrhenius plots" of Figure 6b as a function of $1/T_s$ yield very different slopes which might be interpreted as different "effective barrier heights" dependent on the incident methane translational energy. These observations are simply explained by the requirement for a pooled energy in excess of E_0 for reactions to occur in individual molecule/cluster complexes. As the incident methane translational energy is reduced, the surface degrees of freedom become increasingly important as a source of energy to help overcome the barrier to reaction.

The statistical model was also used to predict the angular distribution of methane from methyl radical hydrogenation on Pt(111) at 240 K via detailed balance.[36] The predicted angular distribution peaks around the surface normal as $\cos^{15} \vartheta$, rather than $\cos^{37} \vartheta$ as observed experimentally. This discrepancy is not too worrisome because the model parameters were based on the only available methane dissociative sticking data taken in the limit of zero coverage, whereas the methyl radical hydrogenation reactions were performed at close to saturation combined coverage of adsorbed H and methyl radicals. Detailed balance calculations should only rigorously apply under identical surface coverage conditions. It seems likely that the sharpening of the experimental methane angular distribution is caused by chemisorbate induced tempering of the surface reactivity. Recently, Matsumoto

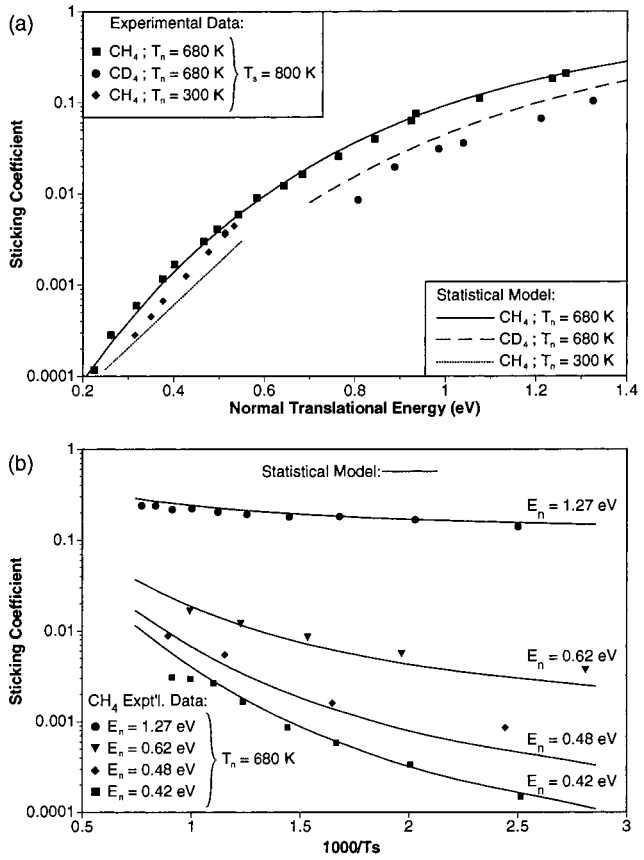

FIGURE 6. Comparison of theoretical simulations[36] of methane dissociative sticking on Pt(111) with data from molecular beam experiments.[35a,37] The three free parameters of the statistical model were fixed once and for all by the CH_4 $T_{nozzle} = 680$ K dissociative sticking coefficient versus normal translational energy data.

and co-workers[38] were able to examine the high-coverage methyl radical hydrogenation on Pt(111) by laser induced thermal reaction (LITR) and claimed the dynamics to be in qualitative, but not quantitative, accord with the zero coverage predictions of the statistical model. Here again, a coverage dependent activation barrier may be responsible for the discrepancies encountered.

When the barrier height for CD_4 dissociative adsorption is raised from its zero coverage value of 0.68 eV to 1.21 eV, detailed balance simulations of the statistical model[39] recover the mean translational energy of $\langle E_T \rangle = 0.43 \pm 0.01$ eV observed for the CD_4 product from LITR. Figure 7 compares the CD_4 translational energy distribution from LITR occurring at a calculated temperature of $T_s = 395$ K with the detailed balance prediction of the statistical model with $E_0 = 1.21$ eV. The maximum translational energy of the CD_4 from LITR, $E_{Tmax} = 1.2 \pm 0.1$ eV, provides an experimental lower bound for the barrier height of the reverse reaction which agrees well with the theoretical estimate based on fitting the observed $\langle E_T \rangle$. The fraction of the exit channel exothermicity that appears in product translation, $f_T = 36\%$, is very similar to that observed for CO oxidation. Detailed balance predictions for the methane angular distributions from the thermally induced methyl radical hydrogenation reactions are given in Figure 8. The increased E_0 barrier height proposed at

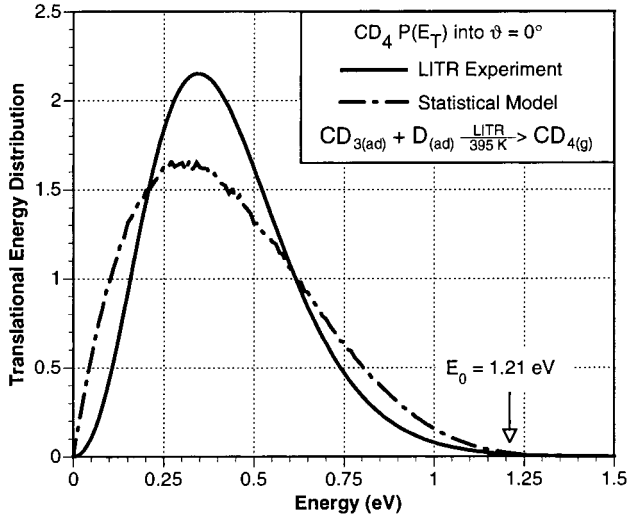

FIGURE 7. Product translational energy distributions for the laser induced thermal reaction $CD_3(ad) + D(ad) \rightarrow CD_4(g)$ assumed to occur at the calculated peak surface temperature of 395 K. The experimental translational energy distribution derived from the best fit to the CD_4 product TOF spectra from Matsumoto's LITR experiments[38] is shown alongside the detailed balance prediction of the statistical model for reaction at 395 K with $E_0 = 1.21$ eV.

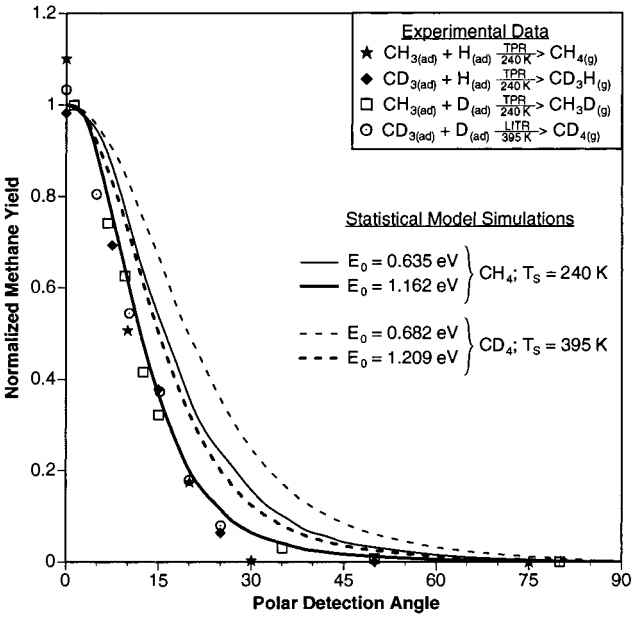

FIGURE 8. Product angular distributions for several thermally induced methyl radical hydrogenation reactions.[34,38] The detailed balance predictions of the statistical model are shown for both the zero coverage dissociative adsorption barrier determined by molecular beam experiments and the high coverage barrier determined by LITR. The variations in E_0 with H/D substitution simply reflect zero-point energy shifts.

high coverage sharpens the methane angular distributions into quite good agreement with experiment. A final comforting feature of the statistical theory is that it predicts a finite mean translational energy for methane desorbing at high angles, rather than the progression to infinite energy as ϑ tends to 90°, as predicted by the more familiar 1-D adsorption/desorption theories.[40] Ultimately, this statistical over-the-barrier model of the $CH_4(g) \leftrightarrow CH_3(ad)$

+ H(ad) reactions is able to predict a remarkably wide range of dynamical behavior in a simple, unified manner.

6. Conclusions

The studies of Pt(111) reactivity highlighted here have revealed a range of phenomena familiar from other phases: ballistic collisions, cage effects, and the persistent utility of transition state theory. The adsorbate photochemical reactions have proven to be useful model systems for investigating the dynamics of catalytic reactions. The important theoretical outcome of this work has been the development of a microcanonical rate theory for direct dissociative adsorption/recombinative desorption reactions which can provide detailed predictions for state resolved sticking and desorption probabilities. In the future, it is anticipated that photochemical methods will provide an increasingly useful complement to molecular beam techniques for probing the reaction dynamics of catalysis. Although much remains to be learned, the basic tools required to experimentally measure and theoretically extract the important features of catalytic potential energy surfaces are sufficiently well-developed at present that the prospects for intelligently designing and optimizing future catalysts seem bright indeed.

This research was made possible by National Science Foundation Grants CHE-9214817 and CHE-9634272 and a talented group of students and postdoctoral fellows to whom I am most grateful.

References

(1) Somorjai, G. *Introduction to Surface Chemistry and Catalysis*; Wiley-Interscience: New York, 1994.
(2) *(2) Dynamics of Gas−Surface Interactions*; Rettner, C. T., Ashfold, M. N. R., Eds.; Royal Society of Chemistry: London, 1991.
(3) Avouris, Ph. Manipulation of Matter at the Atomic and Molecular Levels. *Acc. Chem. Res.* **1995**, *28*, 95−102.
(4) Rettner, C. T.; Auerbach, D. J.; Tully, J. C.; Kleyn, A. W. Chemical Dynamics at the Gas−Surface Interface. *J. Phys. Chem.* **1996**, *100*, 13021−13033.
(5) Rettner, C. T. Dynamics of the Direct Reaction of Hydrogen Atoms Adsorbed on Cu(111) with Hydrogen Atoms Incident from the Gas Phase. *Phys. Rev. Lett.* **1992**, *69*, 383−386.
(6) Benson, S. W. *Thermochemical Kinetics*; Wiley-Interscience: New York, 1976; p 191.
(7) Levine, R. D.; Bernstein, R. B. *Molecular Reaction Dynamics and Chemical Reactivity*; Oxford University Press: New York, 1987.
(8) Harris, J.; Kasemo, B. On Precursor Mechanisms for Surface Reactions. *Surf. Sci.* **1981**, *105*, L281−L287.
(9) Bourdon, E. D. B.; Das, P.; Harrison, I.; Polanyi, J. C.; Segner, J.; Stanners, C. D.; Williams, R. J.; Young, P. A. Photodissociation, Photoreaction and Photodesorption of Adsorbed Species. *Faraday Discuss. Chem. Soc.* **1986**, *82*, 343−358. Harrison, I.; Polanyi, J. C.; Young, P. A. Photochemistry of Adsorbed Molecules. IV. Photodissociation, Photoreaction, Photoejection, and Photodesorption of H_2S on LiF(001). *J. Chem. Phys.* **1988**, *89*, 1498−1523.
(10) Meiher, W. D.; Ho, W. Photochemistry of Oriented Molecules Coadsorbed on Solid Surfaces: The formation of CO_2 + O from Photodissociation of O_2 Coadsorbed with CO on Pt(111). *J. Chem. Phys.* **1989**, *91*, 2755−2756. Meiher, W. D.; Ho, W. Bilmolecular Surface Photochemistry: Mechanisms of CO Oxidation on Pt(111) at 85 K. *J. Chem. Phys.* **1993**, *99*, 9279−9295.
(11) Zhou, X.-L.; Zhu, X.-Y.; White, J. M. Photochemistry at Adsorbate/Metal Interfaces. *Surf. Sci. Rep.* **1991**, *13*, 73−220.
(12) *Laser Spectroscopy and Photochemistry on Metal Surfaces*, Parts I and II; Dai, H.-L., Ho, W., Eds.; World Scientific: Singapore, 1995.
(13) Hasselbrink, E. Photodynamics on Surfaces Revealed by Laser Studies. *Ber. Bunsen-Ges. Phys. Chem.* **1993**, *97*, 1692−1697.
(14) Ho, W. Surface Photochemistry. *Surf. Sci.* **1994**, *299/300*, 996−1007.
(15) Harrison, I. Adsorbate Photochemical Dynamics on Pt(111). Chapter 27 of ref 12.
(16) Ukraintsev, V. A.; Harrison, I. Photoreaction Dynamics of CO Oxidation on Pt(111). *J. Chem. Phys.* **1992**, *96*, 6307−6310.
(17) Ukraintsev, V. A.; Harrison, I. Photochemical Hydrogenation of Methyl Radicals on Pt(111). *J. Chem. Phys.* **1993**, *98*, 5171−5173.
(18) Rettner, C. T.; Mullins, C. B. Dynamics of the Chemisorption of O_2 on Pt(111): Dissociation via Direct Population of a Molecularly Chemisorbed Precursor at High Incidence Kinetic Energy. *J. Chem. Phys.* **1991**, *94*, 1626−1635.
(19) Artsyukhovich, A. N.; Ukraintsev, V. A.; Harrison, I. Low-Temperature Sticking and Desorption Dynamics of Oxygen on Pt(111). *Surf. Sci.* **1996**, *347*, 303−318.
(20) Zhu, X.-Y.; Hatch, S. R.; Campion, A.; White, J. M. Surface Photochemistry. II. Wavelength Dependences of Photoinduced Dissociation, Desorption, and Rearrangement of O_2 on Pt(111). *J. Chem. Phys.* **1989**, *91*, 5011−5020.
(21) Weik, F.; de Meijere, A.; Hasselbrink, E. Wavelength Dependence of the Photochemistry of O_2 on Pd(111) and the Role of Hot Electron Cascades. *J. Chem. Phys.* **1993**, *99*, 682.
(22) Harrison, I.; Ukraintsev, V. A.; Artsyukhovich, A. N. Oxygen Photochemistry on Pt(111). *Proc. SPIE-Int. Soc. Opt. Eng.* **1994**, *2125*, 285−295.
(23) Artsyukhovich, A. N.; Harrison, I. Hot Oxygen Atom Ballistics on Pt(111): Collisional Desorption of Noble Gases. *Surf. Sci.* **1996**, *350*, L199−L204.
(24) Chattering in surface photochemistry is discussed by: Fang, J.-Y.; Guo, H. Multiconfiguration Time-Dependent Hartree Studies of the CH_3I/MgO Photodissociation Dynamics. *J. Chem. Phys.* **1994**, *101*, 5831−5840, and references cited therein.
(25) Wintterlin, J.; Schuster, R.; Ertl, G. Existence of a "Hot" Atom Mechanism for the Dissociation of O_2 on Pt(111). *Phys. Rev. Lett.* **1996**, *77*, 123−126.
(26) Stipe, B. C.; Rezai, M. A.; Ho, W.; Gao, S.; Persson, M.; Lundqvist, B. I. Single Molecule Dissociation by Tunneling Electrons. *Phys. Rev. Lett.* **1997**, *78*, 4410−4413.
(27) Campbell, C. T.; Ertl, G.; Kuipers, H.; Segner, J. A Molecular Beam Study of the Catalytic Oxidation of CO on a Pt(111) Surface. *J. Chem. Phys.* **1980**, *73*, 5862−5873.
(28) Allers, K.-H.; Pfnur, H.; Feulner, P.; Menzel, D. Fast Reaction Products From the Oxidation of CO on Pt(111): Angular and Velocity Distributions of the CO_2 Product Molecules. *J. Chem. Phys.* **1994**, *100*, 3985−3997, and references cited therein.

(29) Coulston, G. W.; Haller, G. L. The Dynamics of CO Oxidation on Pd, Rh, and Pt studied by High-Resolution Infrared Chemiluminescence Spectroscopy. *J. Chem. Phys.* **1991**, *95*, 6932−6944.
(30) Zimmermann, F. M.; Ho, W. State Resolved Studies of Photochemical Dynamics at Surfaces. *Surf. Sci. Rep.* **1995**, *22*, 127−247.
(31) Van Veen, G. N. A.; Mohamed, K. A.; Baller, T.; De Vries, A. E. Photofragmentation of H_2S in the First Continuum. *Chem. Phys.* **1983**, *74*, 261−271.
(32) Since the mean energy for passage over the transition state in a thermal reaction is typically within a few k_bT of E_0: Menzinger, M.; Wolfgang, R. The Meaning and Use of the Arrhenius Activation Energy. *Angew. Chem.* **1969**, *8*, 438−444.
(33) Ukraintsev, V. A.; Long, T. J.; Harrison, I. Photofragmentation Dynamics of Submonolayers of CH_3-Br Adsorbed on Pt(111). *J. Chem. Phys.* **1992**, *96*, 3957−3965. Ukraintsev, V. A.; Gowl, T.; Long, T. J.; Harrison, I. Photoinduced Dissociative Electron Attachment of CH_3Br on Pt(111): The Role of the Local Work Function. *J. Chem. Phys.* **1992**, *96*, 9114−9121.
(34) Ukraintsev, V. A.; Harrison, I. Methane Dissociative Chemisorption on Pt(111) Explored by Microscopic Reversibility. *Surf. Sci.* **1993**, *286*, L571−L576.
(35) Harris, J.; Simon, J.; Luntz, A. C.; Mullins, C. B.; Rettner, C. T. Thermally Assisted Tunneling: CH_4 Dissociation on Pt(111). *Phys. Rev. Lett.* **1991**, *67*, 652−655. Luntz, A. C.; Harris, J. CH_4 Dissociation on Metals: A Quantum Dynamics Model. *Surf. Sci.* **1991**, *258*, 397−426.
(36) Ukraintsev, V. A.; Harrison, I. A Statistical Model for Activated Dissociative Adsorption: Application to Methane Dissociation on Pt(111). *J. Chem. Phys.* **1994**, *101*, 1564−1581.
(37) Luntz, A. C.; Bethune, D. S. Activation of Methane Dissociation on a Pt(111) Surface. *J. Chem. Phys.* **1989**, *90*, 1274−1280.
(38) Watanabe, K.; Lin, M. C.; Gruzdkov, Y.; Matsumoto, Y. Mechanism for the Desorption of Molecularly and Dissociatively Adsorbed Methane on Pt(111) Probed by Pulse-Laser Heating. *J. Chem. Phys.* **1996**, *104*, 5974−5982.
(39) Harrison, I. Unpublished calculations in which only E_0 was varied from the molecular beam determined parameters of ref 36. The full Gibbs distribution was used, and state counting was done via the Beyer−Swinehart algorithm.
(40) Van Willigan, W. Angular Distribution of Hydrogen Molecules Desorbed From Metal Surfaces. *Phys. Lett.* **1968**, *28A*, 80−81. Also see discussion by: Harris, J.; Holloway, S.; Rahman, T. S.; Yang, K. On the Dynamics of the Associative Desorption of H_2. *J. Chem. Phys.* **1988**, *89*, 4427−4439.

AR9700926